Cell Host & Microbe
Article

Host Restriction Factor SAMHD1 Limits Human T Cell Leukemia Virus Type 1 Infection of Monocytes via STING-Mediated Apoptosis

Alexandre Sze,[1] S. Mehdi Belgnaoui,[1] David Olagnier,[2] Rongtuan Lin,[1] John Hiscott,[2,*] and Julien van Grevenynghe[1,2,*]
[1]Lady Davis Institute-Jewish General Hospital, McGill University, Montreal, QC H3T 1E2, Canada
[2]Vaccine and Gene Therapy Institute of Florida, Port St. Lucie, FL 34987, USA
*Correspondence: jhiscott@vgtifl.org (J.H.), julien.vangrevenynghe@mail.mcgill.ca (J.v.G.)
http://dx.doi.org/10.1016/j.chom.2013.09.009

SUMMARY

Human T cell leukemia virus type 1 (HTLV-1) is the causative agent of adult T cell leukemia and HTLV-1-associated myelopathies. In addition to T cells, HTLV-1 infects cells of the myeloid lineage, which play critical roles in the host innate response to viral infection. Investigating the monocyte depletion observed during HTLV-1 infection, we discovered that primary human monocytes infected with HTLV-1 undergo abortive infection accompanied by apoptosis dependent on SAMHD1, a host restriction factor that hydrolyzes endogenous dNTPs to below the levels required for productive reverse transcription. Reverse transcription intermediates (RTI) produced in the presence of SAMHD1 induced IRF3-mediated antiviral and apoptotic responses. Viral RTIs complexed with the DNA sensor STING to trigger formation of an IRF3-Bax complex leading to apoptosis. This study provides a mechanistic explanation for abortive HTLV-1 infection of monocytes and reports a link between SAMHD1 restriction, HTLV-1 RTI sensing by STING, and initiation of IRF3-Bax driven apoptosis.

INTRODUCTION

Infection with human T cell leukemia virus type 1 (HTLV-1) affects approximately 20 million people worldwide (Cook et al., 2013) and is a major cause of mortality and morbidity in endemic areas such as southern Japan, the Caribbean basin, Central/South America, and Western Africa (Ragin et al., 2008). Most infected individuals are asymptomatic carriers of the virus, although they remain at risk for opportunistic infections (Verdonck et al., 2007). Chronic HTLV-1 infection can lead to a number of severe pathologies associated with poor prognosis, including the aggressive adult T cell leukemia (ATL), progressive HTLV-1-associated myelopathy/tropical spastic paraparesis (HAM/TSP), uveitis, and infective dermatitis in children (Cook et al., 2013; Yamano and Sato, 2012). HTLV-1 has a preferential tropism for $CD4^+$ T cells, while both $CD4^+$ and $CD8^+$ T cells constitute viral reservoirs in HAM/TSP patients (Cook et al., 2013). Unlike most retroviruses, cell-free HTLV-1 is poorly infectious and does not stably infect its primary $CD4^+$ T lymphocyte target. Rather, HTLV-1 utilizes various cell-to cell transmission strategies, including transfer of viral assemblies, formation of virological synapses, or formation of intracellular conduits (Igakura et al., 2003; Pais-Correia et al., 2010; Van Prooyen et al., 2010). HTLV-1 also infects cells of the myeloid lineage, which play critical roles in the host innate response to viral infection. Previous studies have shown that cell-free HTLV-1 particles can productively infect DC, which then participate in viral transmission to and transformation of $CD4^+$ T cells (Jones et al., 2008). HTLV-1 infection of DC elicits an early antiviral response mediated by the production of type I interferon (IFN) (Colisson et al., 2010), although the number of peripheral DC, as well as the IFN response, is reduced in chronically infected asymptomatic and ATL subjects (Hishizawa et al., 2004). Monocyte precursors that would normally replenish the DC population are unable to properly differentiate during chronic HTLV-1 infection, and recent evidence indicates monocyte depletion in HTLV-1 infected patients (Makino et al., 2000; Nascimento et al., 2011). The molecular consequences of de novo HTLV-1 infection on host innate immunity in monocytic cells have yet to be elucidated.

Human myeloid and bystander $CD4^+$ T cells are refractory to HIV-1 infection, in part because the host restriction factor SAMHD1 prevents efficient viral DNA synthesis (Baldauf et al., 2012; Descours et al., 2012; Laguette and Benkirane, 2012; Laguette et al., 2011). SAMHD1 functions in nondividing cells as a deoxynucleoside triphosphate triphosphohydrolase, which hydrolyzes the endogenous pool of deoxynucleoside triphosphates (dNTP) to levels below the threshold required for reverse transcription (Ayinde et al., 2012; Goldstone et al., 2011; Lahouassa et al., 2012). SAMHD1 was initially characterized in the context of the autoimmune disorder Aicardi-Goutières syndrome, and genetic mutations that render SAMHD1 nonfunctional result in uncontrolled inflammatory and type I IFN responses against self DNA (Rice et al., 2009). Primary cells from these patients are highly susceptible to HIV-1 infection (Baldauf et al., 2012; Berger et al., 2011; Descours et al., 2012). The Vpx accessory protein of HIV-2 and its counterpart in certain strains of SIV antagonize SAMHD1 by inducing proteasome-dependent degradation (Ayinde et al., 2012; Laguette et al., 2012). HIV-1 restriction mediated by SAMHD1 is overcome by silencing its expression with Vpx or by the addition of exogenous dN (deoxynucleosides) (Baldauf et al., 2012; Descours et al., 2012; Laguette et al., 2011; Lahouassa et al., 2012).

Recognition of evolutionarily conserved molecular structures shared by pathogens, known as pathogen-associated molecular patterns (PAMP), is critical for the initiation of innate immune responses (Kumar et al., 2011). Multiple surface and cytosolic pathogen recognition receptors (PRR) (Kawai and Akira, 2011) have now been identified that sense and respond to microbial infection. Toll-like receptors (TLR) detect distinct PAMP such as lipopolysaccharide (TLR4), single-stranded (ss) and double-stranded (ds) RNA (TLR7/8 and TLR3, respectively), and CpG DNA (TLR9) (Blasius and Beutler, 2010; Kawai and Akira, 2011). The retinoic acid-inducible gene-I (RIG-I)-like receptors (RLR), which include RIG-I and MDA5, represent another PRR family that recognizes cytosolic viral RNA (Blasius and Beutler, 2010; Kawai and Akira, 2011). PRR responsible for the detection of cytosolic DNA include DAI, DDX41, cGAS, and IFI16, all of which trigger IFN production, as well as AIM2 that stimulates an inflammasome-dependent secretion of the proinflammatory IL-1β cytokine (Barber, 2011; Sun et al., 2013). The endoplasmic reticulum resident adaptor STING functions as a DNA sensor for bacterial cyclic GTP (Burdette and Vance, 2013) and mediates detection of viral DNA (Ishikawa and Barber, 2008; Ishikawa et al., 2009; Zhong et al., 2008). STING can also directly complex with ss and ds cytoplasmic viral DNA to initiate antiviral signaling (Abe et al., 2013).

In the present study, we characterized de novo infection of primary human monocytes by HTLV-1 and demonstrated that HTLV-1 infection induces SAMHD1-mediated apoptosis in monocytic cells. We further showed that production of HTLV-1 reverse transcription intermediates (RTI), generated in the presence of SAMHD1, complexed with the innate immune sensor STING and initiated IRF3-Bax-directed apoptosis. These results elucidate the mechanism of HTLV-1 abortive infection of monocytes and link the host restriction factor SAMHD1, the sensing of retroviral RTI by STING, and the initiation of IRF3-Bax-driven apoptosis.

RESULTS

Abortive Infection of Primary Monocytes by HTLV-1 Activates Type I IFN Response

To characterize the impact of HTLV-1 infection on the host antiviral response in primary human monocytes, we first assessed the percentage of HTLV-1-infected monocytes at 3 hr postinfection (hpi), using increasing concentrations of purified HTLV-1 (0–5 μg/ml). Virus binding to monocytes was dependent on the quantity of HTLV-1, as illustrated by surface staining with anti-Env (gp46) monoclonal antibodies (Figure 1A); for subsequent experiments, an HTLV-1 concentration of 2 μg/ml was used, since >90% of the cells displayed virus binding (Figure 1A) (91.7 ± 4.8% $gp46^+$ cells; $p > 0.05$; $n = 5$). HTLV-1 particles were efficiently internalized by monocytes, as determined by intracellular HTLV-1 viral RNA (vRNA) detection at 3 hpi, with the viral RNA load gradually decreasing over the 120 hr time course (Figure 1B). HTLV-1 internalization was further demonstrated by intracellular staining (ICS) for the viral matrix protein p19 at 24 hpi (Figure 1C, blue histograms) (86.7 ± 6.2% of $p19^+$ monocytes; $p < 0.01$ compared to uninfected cells; $n = 5$). Importantly, viral binding and internalization were eliminated by pretreating HTLV-1 with anti-gp46 neutralizing mAb or pretreating monocytes with 0.1% trypsin (Jones et al., 2005) (Figure 1C) ($p < 0.01$ compared to infected cells). The absence of intracellular Tax protein and virion release indicated that monocytes were not productively infected by HTLV-1 (Figure 1C and Figure S1, respectively). Monocyte-derived DC, on the other hand, were productively infected with HTLV-1 (40.6 ± 5.7% Tax^+ cells at 24 hpi) (data not shown).

Despite the nonproductive infection by HTLV-1, monocytes generated a robust innate immune response, as illustrated by the induction of multiple parameters of antiviral signaling. An early increase in phosphorylated interferon regulatory factor 3 (P-IRF3) was detected at 3 hpi (Figure 1D), while increased expression of STAT1, phosphorylated STAT1 (P-STAT1), interferon-stimulated gene 56 (ISG56), and RIG-I were observed at 24 and 48 hpi.

HTLV-1-Infected Monocytes Undergo Apoptosis

We next evaluated the level of apoptosis in HTLV-1-infected $CD14^+$ monocytes by Annexin-V staining. At 24 hpi, infected monocytes displayed higher levels of apoptosis than uninfected cultures (Figure 2A) (22.9 ± 3.5% versus 8.6 ± 1.3%, respectively; $p < 0.01$; $n = 5$), and by 72 hr the percentage of HTLV-1 infected apoptotic cells increased to over 45%. Infection of monocytes with a low dose of HTLV-1 (0.1 μg/ml) also resulted in apoptosis in the $p19^+$ population (Figure S2A). Apoptosis was accompanied by the generation of cleaved caspase-3 (Figure 2B and Figure S2B) (33.4 ± 12.3% and 11.4 ± 2%, for HTLV-1-infected and uninfected cells, respectively; $p < 0.01$; $n = 5$) and loss of mitochondrial potential as shown by reduced $DiOC_6(3)$ intensity (Figure 2C and Figure S2C) ($p < 0.01$; $n = 5$). The pan-caspase inhibitor Z-VAD or the blocking α-gp46 mAb prevented $_{CL}$caspase-3-mediated apoptosis (Figure 2B) and mitochondrial depolarization (Figure 2C). Z-VAD did not interfere with the internalization of HTLV-1, as detected by measuring intracellular p19 (Figure 2B, blue histograms) ($p > 0.05$; $n = 5$). A strong statistical correlation between (1) caspase-3 activation and (2) mitochondrial depolarization and apoptosis was confirmed by the nonparametric Spearman test (Figure 2D) ($r = 0.7845$ and 0.9036, respectively, for 1 and 2; $p < 0.0001$; $n = 25$). Expression of mitochondrial pro- and antiapoptotic molecules were also analyzed; increased Bax expression and caspase-9 cleavage were observed in infected monocytes (Figure 2E) ($p < 0.05$ and $p < 0.01$, respectively; $n = 3$), while expression of Bcl-2 family members Bim, Noxa, Bcl-2, and Mcl-1 were unchanged. In the above experiments, we did not observe death by necrosis or an effect of necrostatin-1 on infected monocytes (Figure S2D). Cleaved caspase-1 and bioactive IL-1β were detected after infection, indicating activation of the inflammasome (Figure S2E). To investigate caspase-1-associated pyroptosis, HTLV-1-infected cells were treated with YVAD, a selective inhibitor of caspase-1; a minor but significant improvement of cell survival was observed (Figure S2F).

A Requirement for SAMHD1 in HTLV-1-Driven Apoptosis in Infected Monocytes

The above observations, detailing abortive HTLV-1 infection of monocytes, are reminiscent of the consequences of host restriction by SAMHD1 during HIV-1 infection (Baldauf et al., 2012; Descours et al., 2012; Doitsh et al., 2010; Laguette et al.,

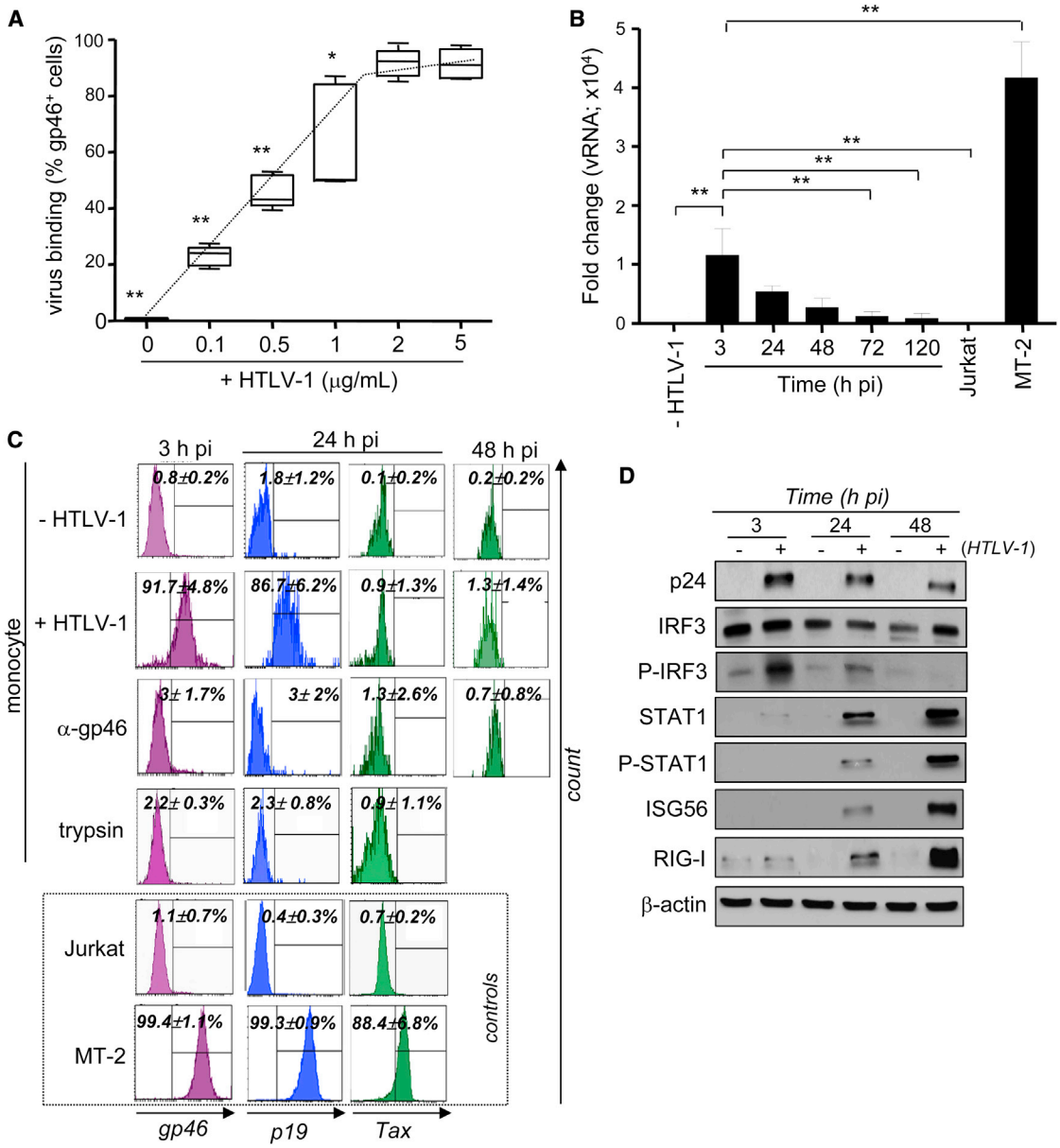

Figure 1. Abortive Infection of Monocytes by HTLV-1 Activates an Antiviral Response

(A–C) Purified monocytes were infected with HTLV-1 for 3 hr and then cocultured with the autologous CD14^{neg} PBMCs for 120 hr pi. (A) Virus binding to monocytes at 3 hpi in response to various HTLV-1 concentrations, analyzed by flow cytometry with anti-gp46 Abs. P values were determined based on the comparison with cells infected with 5 μg/ml HTLV-1 (n = 5). (B) At 3–120 hpi, total RNA was extracted and analyzed for HTLV-1 viral load using primers located in the 5′ UTR of HTLV-1 genome (Table S1). Equivalent vRNA amounts were normalized to β-actin mRNA and calculated as fold change from the level of uninfected monocytes (arbitrary set as 1). Jurkat and MT-2 cells were used as negative and positive control, respectively (n = 5). (C) At 3, 24, and 48 hpi, levels of HTLV-1 binding, viral internalization, and de novo production of viral proteins were assessed by gp46 surface staining, p19, and Tax ICS, respectively. Histograms are representative of raw data from five independent experiments. The mean relative expressions ± SD for all conditions are indicated. MT-2 and Jurkat cells were used as positive and negative controls for all staining, respectively.

(D) p24 expression and type I IFN responses were examined by immunoblotting (n = 3). See also related Figure S1.

2011), prompting us to investigate whether SAMHD1 functioned similarly to restrict HTLV-1 infection. Small interfering RNA (siRNA)-mediated silencing of SAMHD1 resulted in a 72 ± 11.8% reduction in SAMHD1 expression (Figure 3A), but did not alter HTLV-1 internalization in control or siRNA-transfected monocytes (>95.5%) (Figure 3B, right histograms). Following HTLV-1 infection, induced apoptosis was also reduced by ~70% in SAMHD1-silenced monocytes compared to control siRNA-treated monocytes (Figure 3B) ($p < 0.01$; n = 5). The correlation between inhibition of SAMHD1 expression and inhibition of HTLV-1-induced apoptosis in primary monocytes was significant (Figure 3C) (r = 1; p = 0.0167; n = 5, Spearman test).

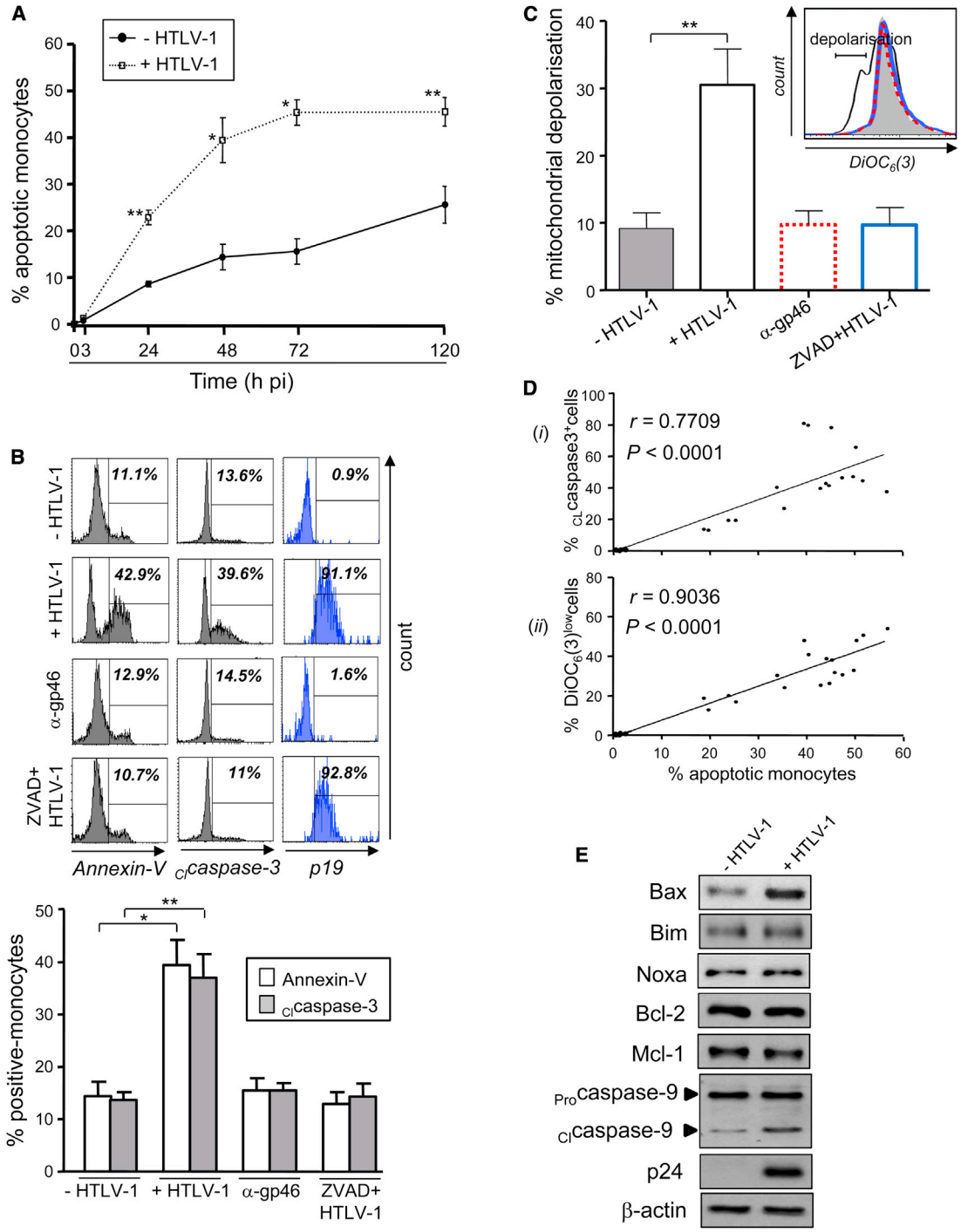

Figure 2. HTLV-1-Infected Monocytes Undergo Mitochondrial-Dependent Apoptosis

(A) The percentage of apoptosis on gated $CD3^{-}CD14^{+}$monocytes was assessed by Annexin-V staining at 3–120 hpi. P values were determined by the comparison with uninfected cells (n = 5).

(B) Levels of Annexin-V, $_{CL}$caspase-3, and p19 expression determined at 48 hpi, treated or not with Z-VAD or with α-gp46 mAb. Representative histograms from five independent experiments are shown above. Data are represented as mean ± SD.

(C) At 48 hpi, the loss of mitochondrial membrane potential in the presence or absence of Z-VAD or α-gp46 mAb was evaluated by flow cytometry using the fluorescent dye $DiOC_6(3)$. Results shown represent the percentage of $CD3^{-}CD14^{+}DiOC_6(3)^{low}$ monocytes, as indicated above in the representative histograms (n = 5).

(D) The correlations between the percentage of apoptotic monocytes and (1) $_{CL}$caspase-3 expression or (2) mitochondrial depolarization were calculated in infected monocytes during the course of the coculture (n = 25; Spearman test).

(E) Expression levels of p24, Bcl-2 family members, and caspase-9 cleavage were assessed by immunoblotting at 3 hpi (n = 3). Data are represented as mean ± SD. See related Figure S2.

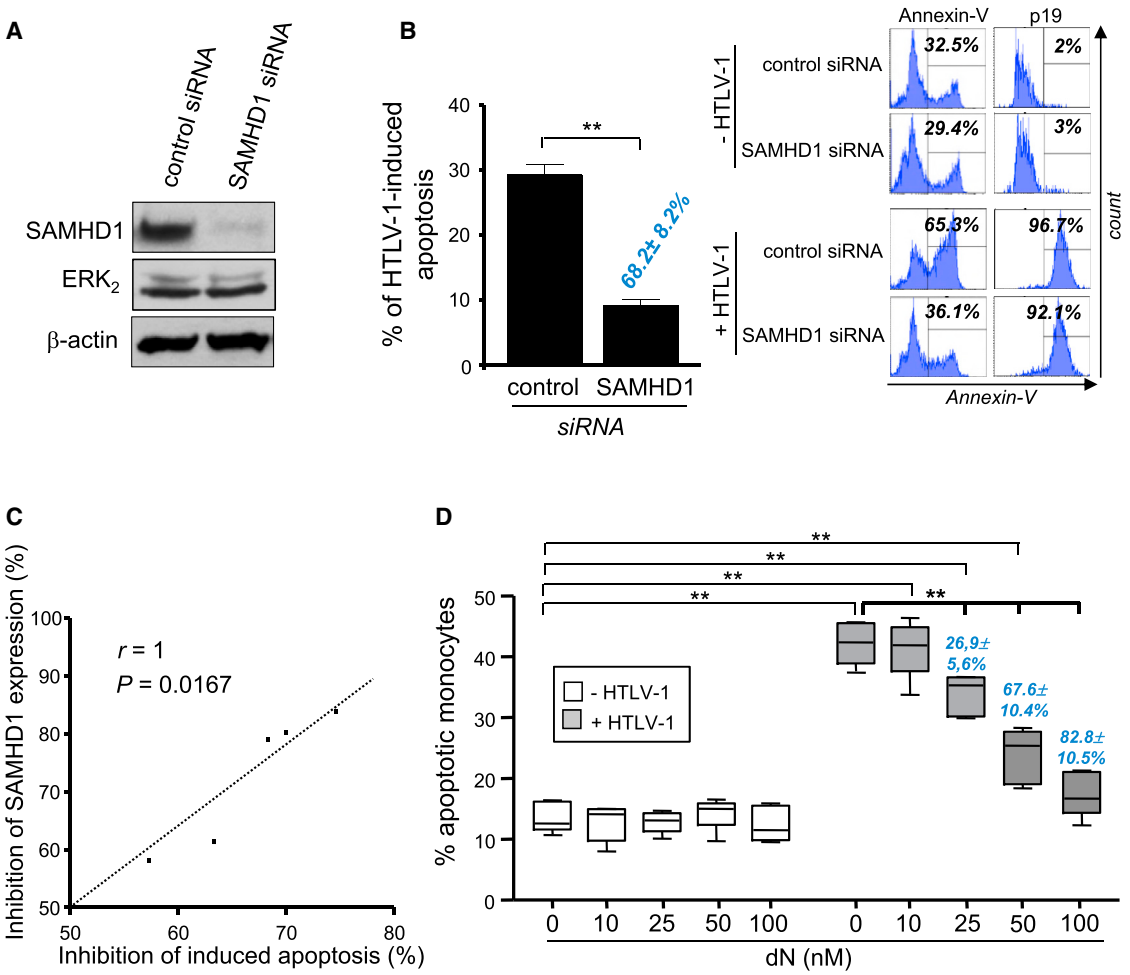

Figure 3. SAMHD1 Drives Apoptosis in HTLV-1-Infected Monocytes

(A–C) Monocytes were transfected with control or SAMHD1 siRNA for 72 hr, and then infected with HTLV-1 for 48 hr. (A) Efficiency of SAMHD1 silencing was determined at day 3 by immunoblotting (n = 5). No changes were observed in total ERK_2 expression. (B) Levels of apoptosis and intracellular p19 on transfected $CD14^+$ monocytes at 48 hpi. Results represent the HTLV-1-induced apoptosis determined on transfected monocytes using the formula: % of apoptosis in infected cells − % of apoptosis in uninfected cells. Data are expressed as mean ± SD for five independent experiments, including the inhibition of apoptosis (%) when SAMHD1 was silenced. Flow histograms on the right are representative of raw data. (C) Correlation between the inhibition of SAMHD1 expression and HTLV-1-induced apoptosis determined on transfected monocytes (n = 5 [values from (A) and (B)]; Spearman test).

(D) Levels of apoptosis determined in the presence of increasing doses of exogenous dN at 48 hpi. Percentage of apoptosis inhibition determined in the presence of dN are also indicated in blue. Statistical analyses are based on the comparison to untouched monocytes, except for those indicated in bold, that are calculated when compared to HTLV-1-infected, non-dN-treated monocytes (n = 5). Data are represented as mean ± SD. See related Figure S3.

The deoxynucleoside triphosphate triphosphohydrolase function of SAMHD1 blocks reverse transcription of retroviral RNA by depleting the dNTP pool required for complete reverse transcription (Ayinde et al., 2012; Goldstone et al., 2011; Hollenbaugh et al., 2013; Kim et al., 2012; Lahouassa et al., 2012), an effect reversed by the addition of exogenous dN (Lahouassa et al., 2012). To explore the relationship between the triphosphohydrolase activity of SAMHD1 and apoptosis, primary monocytes were infected with HTLV-1 in the presence of increasing concentrations of exogenous dN (0–100 nM). SAMHD1-mediated apoptosis was inhibited by addition of exogenous dN in a dose-dependent manner (Figure 3D), with apoptosis reduced to control levels in monocytes treated with 100 nM dN (>80% inhibition of apoptosis). We did not observe de novo Tax expression following SAMHD1 knockdown or dN treatment in infected monocytes at 48 hpi (n = 3; data not shown). These results demonstrate that nucleotide pool depletion, mediated by SAMHD1 function, correlates directly with HTLV-1-induced apoptosis.

HTLV-1-Induced Apoptosis Correlates with the Generation of Cytosolic RTI

Previous studies demonstrated that incomplete synthesis of retroviral DNA triggered a proapoptotic response in HIV-1-infected bystander $CD4^+$ T cells (Doitsh et al., 2010). To assess the presence of RTI in HTLV-1-infected monocytes, viral DNA was measured in total versus nuclear fractions at 3–120 hpi; HTLV-1 RTI were detected only in the total fraction (Figure 4A and Figures S3A and S3B), indicating that viral DNA synthesis was initiated in the cytosol, but was not fully reverse transcribed

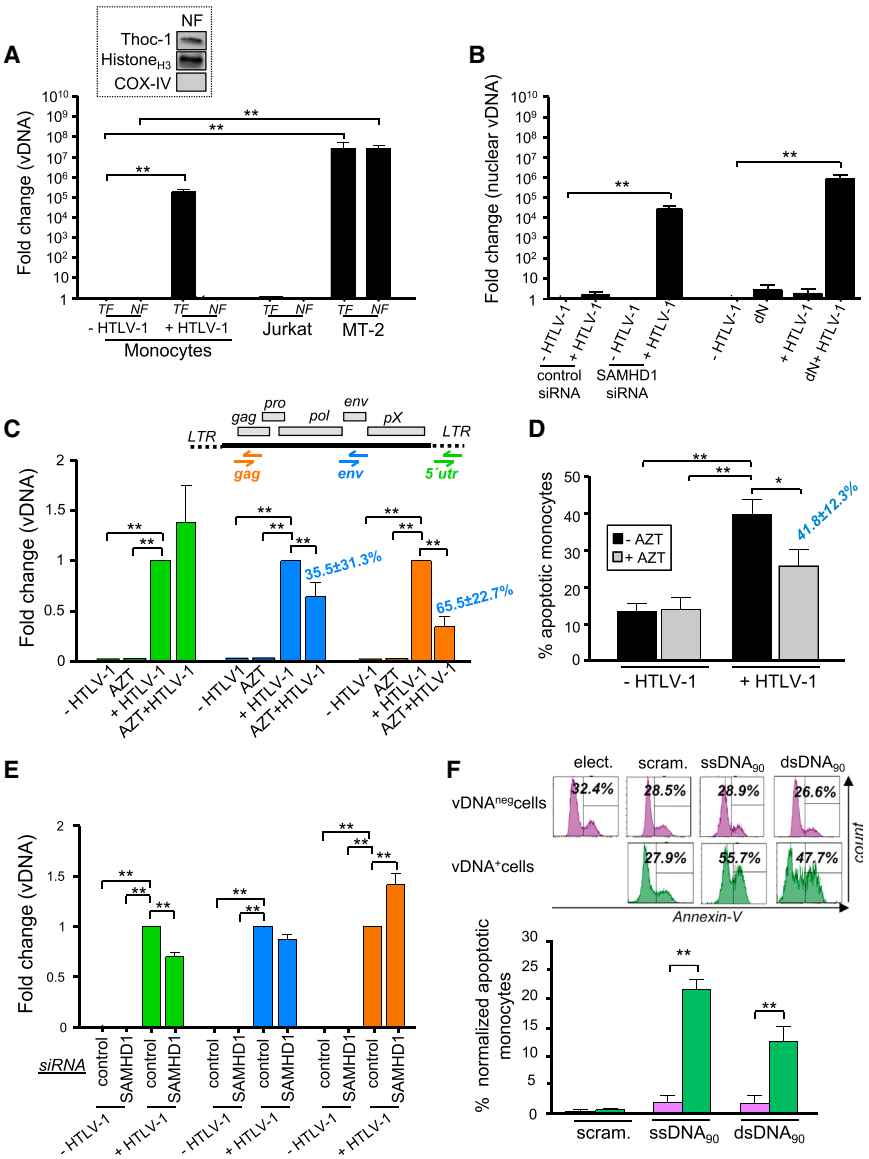

Figure 4. Cytosolic RTI Induce Monocyte Apoptosis Following HTLV-1 Infection

(A) At 24 hpi, DNA was extracted from total (TF) and nuclear (NF) fractions in monocytes. Viral load was determined by qPCR using 5′ UTR primers and normalized to erv-3. Results shown represent the relative fold change and statistical analyses, compared to uninfected monocytes (n = 5). Purity of NF was determined by immunoblotting using antibodies against nuclear (Thoc-1 and Histone$_{H3}$) and cytosolic (COX-IV) proteins.

(B) Monocytes were transfected with SAMHD1 siRNA, treated with exogenous 100 nM dN, then treated as in (A). Results represent relative fold change compared to uninfected cells, treated with control siRNA (n = 5).

(C) Fold change of vDNA was determined at 48 hpi using several primer pairs, relative to infected monocytes without AZT.

(D) Inhibition of apoptosis mediated by AZT is indicated in blue.

(E) Fold change of vDNA performed in monocytes expressing or not SAMHD1 at 24 hpi using several primer pairs. Data are in (C) and (D) are represented as mean ± SD.

(F) The addition of HTLV-1 RTI in monocytes initiates apoptosis. Purified monocytes were transfected with HTLV-1 ss or dsDNA$_{90}$ or scrambled ssDNA. At 48 hr, cells were labeled with Annexin-V-V450, CD14-APC H7, and streptavidin-APC. Streptavidin-APC ICS distinguished between monocytes that were vDNA^{neg} (purple) or vDNA^{+} cells (green) in the same sample. Elect. = electroporated only; scram. = scrambled ssDNA$_{90}$. Values represent the percentages of normalized apoptosis indicated by the formula: % of apoptosis in RTI-transfected monocytes with siRNA − % of apoptosis in electroporated-only cells. Apoptosis resulting from electroporation averaged between ~15% and 19%. Flow histograms are representative of raw data from five independent experiments. See related Figure S3.

and did not reach the nucleus (Nisole and Saïb, 2004). Silencing SAMHD1 expression or treatment with exogenous dN led to the detection of HTLV-1 DNA in the nucleus, as well as integrated provirus, in infected monocytes (Figure 4B and Figure S3C).

Several primer pairs were designed to monitor sequential steps in HTLV-1 reverse transcription, including strong-stop DNA (*5′utr*), and DNA elongation (*env* or *gag*) (Figure 4C, upper schematic, and Table S1) (Doitsh et al., 2010). Primary monocytes were treated with 5μM azidothymidine (AZT), a nucleoside analog reverse transcriptase inhibitor that prevents elongation of reverse-transcribed DNA after initiation (Doitsh et al., 2010), and then infected with HTLV-1. AZT treatment had no inhibitory effect on the initiation of HTLV-1 reverse transcription (Figure 4C), as detected with the *5′utr* primers (green), whereas DNA strand elongation was progressively inhibited, as detected using *env* (blue) and *gag* (orange) region-specific probes (Figure 4C) (35.5 ± 31.3% and 65.5 ± 22.7% inhibition, respectively; $p < 0.01$; n = 5). Following HTLV-1 infection, apoptosis in monocytes treated with AZT was reduced by >40% compared to infected cells without AZT (Figure 4D) (41.8 ± 12.3%; $p < 0.05$; n = 5). These results demonstrate that AZT blocked HTLV-1 DNA elongation and suggested that cytosolic RTI generation was linked with virus-mediated apoptosis. These primers were also used in the context of SAMHD1 silencing, to investigate the production of early- versus late-stage RTI. SAMHD1 knockdown led to a decrease in the generation of total and early transcripts (green [*5′utr*]; 1.45 ± 0.41-fold decrease), concomitant with an accumulation of late reverse transcription products (orange [*gag*]; 1.39 ± 0.27-fold increase) (Figure 4E).

To determine if HTLV-1 RTI directly mediated apoptosis, synthetic ss or ds 90 nt HTLV-1 DNA (vDNA), conjugated with biotin, were introduced into primary monocytes. Monocytes harboring HTLV-1 ss or dsDNA$_{90}$ (vDNA^{+} cells; green histograms) underwent apoptosis (59.2 ± 3.5% and 48.9 ± 6.9%, respectively), whereas vDNA-free monocytes did not undergo apoptosis (purple histograms; ~30% apoptosis in cells electroporated only, or

transfected with digested ssDNA$_{90}$ [data not shown]) (Figure 4E). The transfection of monocytes with scrambled RTI (whose sequence was generated by randomizing the U5 sequence) did not result in apoptosis, confirming the specificity of HTLV-1 RTI to induce apoptosis (Figure 4F). Overall, these results provide evidence for a direct contribution of cytosolic RTI to HTLV-1-induced apoptosis.

HTLV-1 RTI Signal via STING to Induce Apoptosis and the IFN Response

The endoplasmic reticulum resident transmembrane sensor STING (stimulator of interferon genes) is central to the generation of an innate immune response, through its capacity to directly bind viral and bacterial DNA (Abe et al., 2013; Burdette and Vance, 2013; Ishikawa and Barber, 2008; Ishikawa et al., 2009). Given the importance of STING, we next examined whether STING could recognize and complex with HTLV-1 RTI. Using streptavidin beads to pull down biotinylated HTLV-1 DNA, we demonstrated that STING was precipitated from primary monocytes via interactions with ss or dsDNA$_{90}$ (Figure 5A). Furthermore, the formation of the complex between STING and HTLV-1 DNA was associated with the induction of type I IFN signaling and apoptosis, as illustrated by increased expression of RIG-I, ISG56, and Bax (Figure 5A) ($p < 0.01$; $n = 3$). Transfection of monocytes with scrambled RTI resulted in STING pull-down and the induction of ISGs. However, no increase in Bax expression was observed in these cells. No complex formation was observed between HTLV-1 RTI and the RNA sensor RIG-I (Figure 5A).

To determine whether cytosolic detection of HTLV-1 RTI by STING was involved in triggering apoptosis, STING-specific siRNA was introduced into primary monocytes, resulting in ~65% inhibition of STING expression (Figure 5B) ($p < 0.01$; $n = 5$). Knockdown of STING in primary monocytes resulted in a significant improvement in cell survival. In multiple experiments, a 55%–60% inhibition of apoptosis was observed (Figure 5C) ($p < 0.01$ compared to control siRNA-treated cells; $n = 5$), whereas silencing of RIG-I had no effect on HTLV-1-induced apoptosis (Figures S4). A positive correlation between the inhibition of STING expression and HTLV-1-induced apoptosis was established using the nonparametric Spearman test (Figure 5D) ($r = 1$; $p = 0.0167$; $n = 5$). Altogether, these results indicate that HTLV-1 RTI, generated in primary monocytes in a SAMHD1-dependent manner, complex with the DNA sensor STING and initiate apoptosis.

HTLV-1 RTI Trigger Mitochondrial Apoptosis through IRF3-Bax Signaling

HTLV-1 infection of monocytes stimulated IRF3 activation and induction of proapoptotic Bax (Figures 1D and 2E), suggesting that HTLV-1 may trigger apoptosis via a mechanism involving the formation of a proapoptotic complex between IRF3 and Bax (Chattopadhyay et al., 2010, 2011). To determine whether STING recognition of HTLV-1 RTI could trigger apoptosis through IRF3-Bax signaling, we measured Bax and ISG expression as well as IRF3 phosphorylation in infected monocytes knocked down for STING expression. All parameters—Bax, P-IRF3, RIG-I, and ISG56 expression—were inhibited, 95.1 ± 8.5%, 72.1 ± 13.3%, 66.2 ± 48%, and 64.5 ± 29.3%, respectively, by STING knockdown ($p < 0.01$ compared to infected cells treated with control siRNA; $n = 3$) (Figure 6A), thus supporting a role for STING in regulating both the antiviral and apoptotic responses. Similarly, we observed a 73 ± 15.8% inhibition of Bax-expressing monocytes when STING was silenced (Figure S5). As with de novo HTLV-1 infection, the addition of cytosolic ss or dsDNA$_{90}$ led to increased Bax expression (Figure 6B, input blots) ($p < 0.05$; $n = 3$). Both HTLV-1 infection and addition of biotinylated ss or dsDNA$_{90}$ resulted in the generation of a complex between IRF3 and Bax (Figure 6B), whereas no IRF3-Bax complex was observed in monocytes transfected with scrambled RTI. The formation of this proapoptotic complex required both SAMHD1 and STING expression, since RNAi-mediated silencing of either target not only decreased Bax expression, but also abrogated physical association between IRF3 and Bax (Figure 6C).

Next, a multi-parametric antibody cocktail was generated to measure the levels of Annexin-V, Bax, and DiOC$_6$(3) costaining on gated CD14$^+$ monocytes. Infected monocytes expressing Bax (red subset) displayed higher levels of mitochondria depolarization and Annexin-V costaining, compared to the green Bax^{neg} cells (Figure 6D) (74.3 ± 24.8% and 34.3 ± 5.9% DiOC$_6$(3)^{low} Annexin-V$^+$ cells, respectively; $p < 0.01$; $n = 5$). Furthermore, siRNA-mediated silencing of Bax expression reduced the level of apoptosis by ~60%, thus confirming the involvement of Bax in HTLV-1 driven monocyte cell killing (Figure 6E).

HIV-1 DNA Recognition by STING Induces a Proapoptotic Response

Finally, we examined whether STING-mediated recognition of RTI corresponding to strong-stop HIV-1 DNA also led to monocyte depletion through IRF3-Bax driven apoptosis. HIV-1 ssDNA$_{90}$ RTI was introduced into primary monocytes for 3 hr; IRF3 phosphorylation and Bax expression were increased ~7- to 10-fold with the HIV-1 RTI (Figure 7A) ($p = 0.0053$ and $p = 0.0115$, respectively, compared to RTI-free monocytes; $n = 3$). Biotinylated HIV-1 ssDNA$_{90}$ and STING, but not RIG-I, were also pulled down in association with HIV RTI (Figure 7B). As with HTLV-1, the addition of biotinylated HIV-1 ssDNA$_{90}$ resulted in the generation of a heterodimeric IRF3-Bax complex (Figure 7C) and monocytes containing HIV-1 RTI also displayed significantly higher levels of mitochondria-dependent apoptosis (Figure 7D). Overall, these data demonstrate that retroviral RTI recognition by STING induces mitochondria-dependent apoptosis via the formation of the proapoptotic IRF3-Bax heterodimer (Figure S6).

DISCUSSION

In this study, we demonstrate that de novo HTLV-1 infection initiates an abortive infection of primary monocytes and triggers mitochondrial depolarization and caspase-3-dependent cell death. HTLV-1 infection also stimulated induction of a type I IFN response, mediated through IRF3 activation, and triggering of Jak-STAT1 signaling. HTLV-1-induced apoptosis in monocytes was dependent on the triphosphohydrolase activity of SAMHD1, since silencing its expression or the introduction of exogenous dN in HTLV-1-infected monocytes significantly

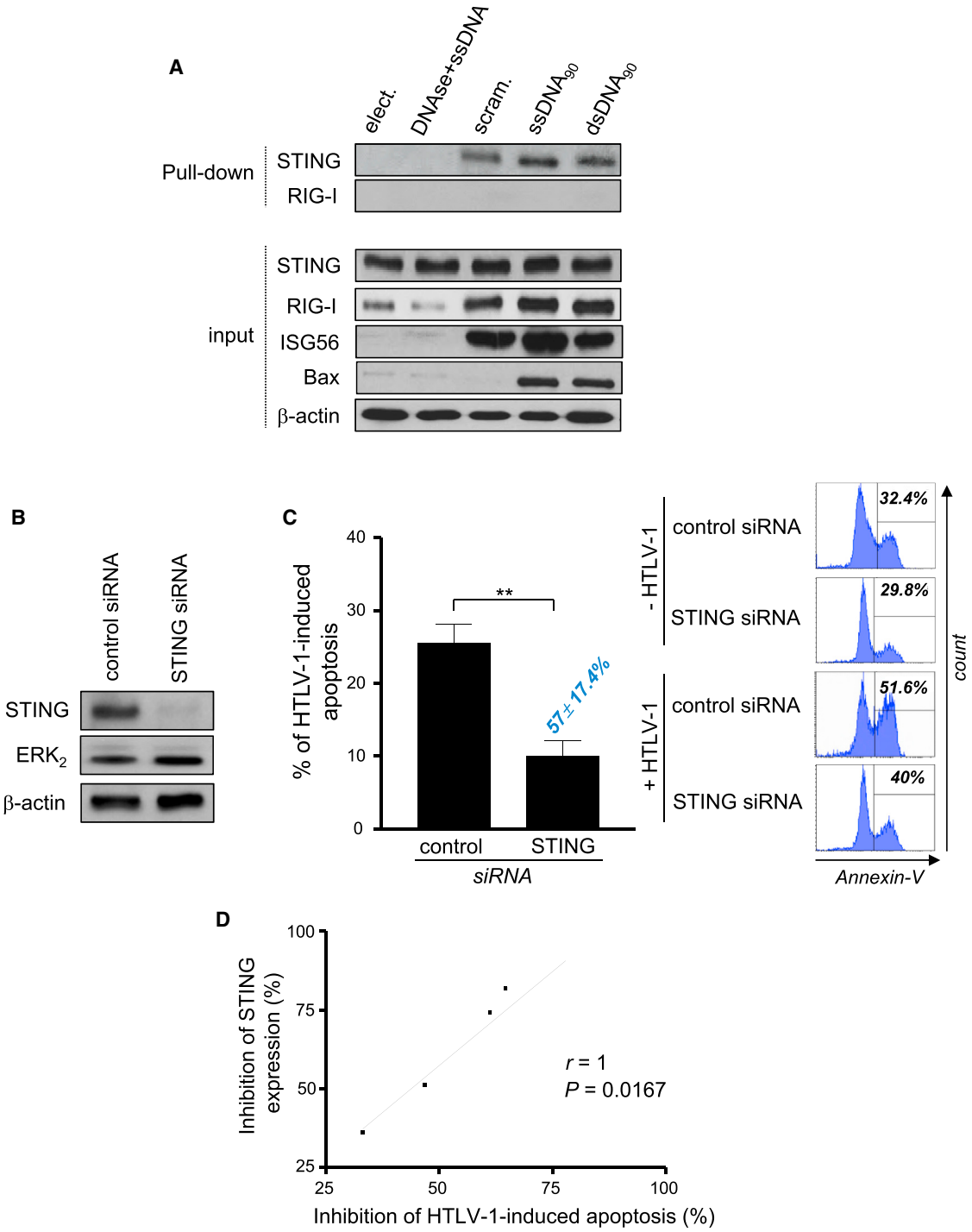

Figure 5. STING Complex Formation with HTLV-1 DNA Induces Apoptosis in Monocytes

(A) Monocytes were transfected with HTLV-1 ss or dsDNA$_{90}$ or scrambled ssDNA for 6 hr; as a negative control, 1 μg HTLV-1 ssDNA was incubated with 1 μl DNase (Ambion) for 1 hr at 37°C. STING and RIG-I pull-down were performed from monocyte lysates via interactions with biotinylated DNA (Experimental Procedures). Input lysates were also analyzed by immunoblot for STING, Bax, β-actin, and ISG expression (n = 3).

(B–D) STING regulates the premature death of infected monocytes. Purified monocytes were transfected with STING siRNA for 72 hr and (B) the efficiency of STING silencing was determined via immunoblotting. (C) Annexin-V staining was determined on transfected CD14$^+$ monocytes at 48 hpi. Values represent the % HTLV-1-induced apoptosis as determined by the formula: % apoptosis in infected cells − % apoptosis in uninfected cells. Inhibition of HTLV-1-mediated apoptosis following STING silencing is indicated in blue. Flow histograms shown on the right side are representative of raw data from five independent experiments. Data are represented as mean ± SD. (D) Correlation between inhibition of STING expression and HTLV-1-mediated apoptosis on transfected monocytes (n = 5; Spearman test). See related Figure S4.

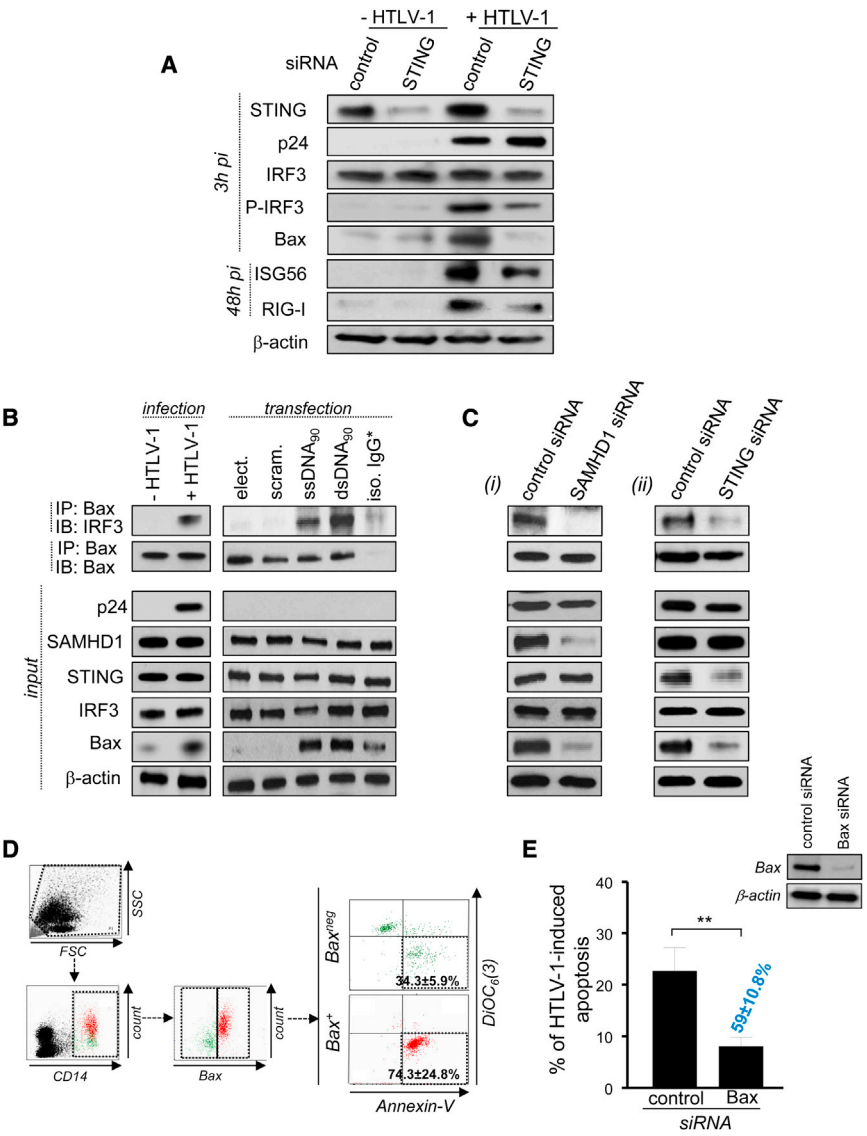

Figure 6. STING Activation Leads to the Formation of an IRF3-Bax Complex

(A) Monocytes were transfected with STING siRNA, and expression of viral and host proteins (p24, STING, Bax, ISG, and p-IRF3) was determined by immunoblotting at 3 and 48 hpi. Representative blots from three independent experiments are shown.

(B and C) Anti-Bax co-IPs were performed at 6 hpi (B) following in vitro infection or transfection with HTLV-1 DNA or (C) in the context of (1) SAMHD1 and (2) STING silencing. Inputs were also analyzed for the expression of several proteins. * = crosslinked isotype IgG_1 antibody (iso. IgG) used during co-IP as negative control; performed on monocytes transfected with $ssDNA_{90}$.

(D) At 24 hpi, a multi-parametric antibody cocktail with $DiOC_6(3)$ dye, Annexin-V-V450, anti-CD14-APC H7, and anti-Bax-APC antibodies was used on cocultured monocytes (n = 5). Anti-Bax antibody was conjugated to Alexa-647 dye using the Zenon mouse IgG_1 labeling kit. Isotype IgG_1 control was used to determine Bax expression. Results represent a flow cytometry gating strategy based on HTLV-1-infected monocytes transfected with control siRNA. Bax^{neg} (green) versus Bax^{+} monocytes (red) were analyzed for mitochondrial depolarization and apoptosis. Percentages of $DiOC_6(3)^{low}$Annexin-V^{+} cells were indicated for both subsets. Data are represented as mean ± SD.

(E) Monocytes were transfected with Bax siRNA for 3 hr prior to HTLV-1 infection. Levels of HTLV-1-induced apoptosis were then investigated at 48 hpi. Results are expressed as mean ± SD for three independent experiments; included in blue is the inhibition of apoptosis during Bax silencing. Bax knockdown was confirmed by immunoblotting 48 hpi. Data are represented as mean ± SD. See related Figure S5.

reduced apoptosis. HTLV-1 RTI were detected exclusively in the cytoplasm of infected monocytes, and it was only after inhibition of SAMHD1 expression that HTLV-1 DNA was detected in the nucleus. The presence of RTI in the cytoplasm was sensed by the ER resident DNA sensor STING. Because of the involvement of STING in the type I IFN response, we examined the fate of IRF3 and detected the formation of an IRF3-Bax complex, which was responsible for the mitochondrial depolarization and apoptosis. These experiments provide a mechanistic explanation for abortive retroviral infection of monocytes and establish a link between SAMHD1 restriction, sensing of retroviral RTI by STING, and the initiation of IRF3-Bax-induced apoptosis. The scope of these observations was further extended by the demonstration that HIV-1 RTI also complexed with STING and triggered apoptosis in the same manner (summarized in Figure S6).

The analogy between the current results and restriction of HIV-1 by SAMHD1 is striking, and several studies have detailed the capacity of SAMHD1 to limit HIV-1 replication in quiescent $CD4^{+}$ T cells and myeloid cells (Baldauf et al., 2012; Descours et al., 2012; Laguette and Benkirane, 2012; Laguette et al., 2011). Prior to the characterization of the role of SAMHD1, Doitsh et al. had demonstrated that abortive HIV-1 reverse transcription in resting tonsil $CD4^{+}$ T cells resulted in apoptotic cell death, triggered by the accumulation of incomplete HIV-1 reverse transcripts (Doitsh et al., 2010). It has since become clear that SAMHD1 is involved in restricting HIV-1 reverse transcription through its dNTP triphosphohydrolase activity, which depletes the intracellular pool of dNTP (Ayinde et al., 2012; Goldstone et al., 2011; Lahouassa et al., 2012). The intracellular dNTP pool appears to be an important rate-limiting factor for retroviral reverse transcription, and SAMHD1 critically modulates this process. SAMHD1 is highly active in monocytes that have low levels of intracellular dNTP (Kaushik et al., 2009; Triques and Stevenson, 2004). In the presence of active SAMHD1, nuclear or integrated HTLV-1 DNA was never detected in infected monocytes, whereas SAMHD1 silencing or restoration of the dNTP pool resulted in the inhibition of virus-induced apoptosis, as well as completion of vDNA synthesis and nuclear translocation. Similarly, reduction of cytoplasmic HTLV-1 RTI levels by AZT also improved cell viability. To investigate directly a role for RTI in

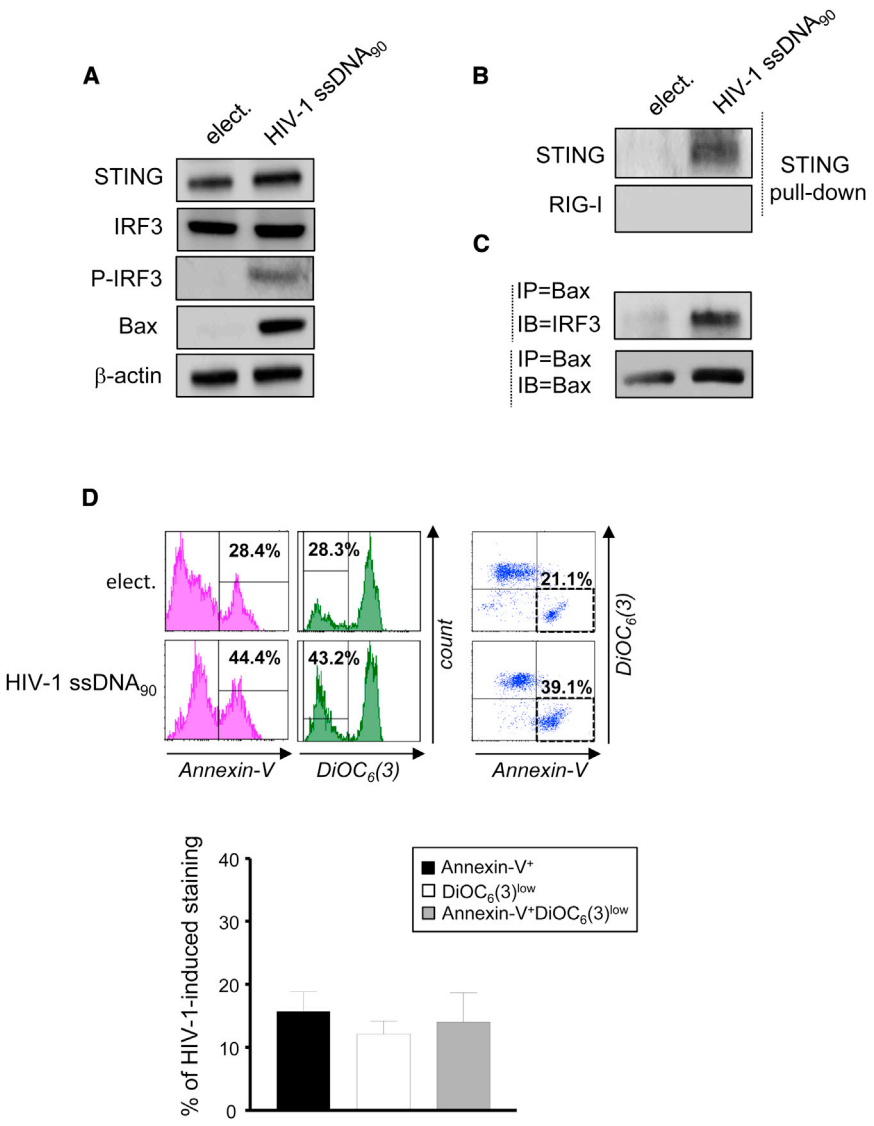

Figure 7. STING Recognition of HIV-1 RTI Leads to IRF3-Bax Interaction and Mitochondrial-Dependent Apoptosis

(A) Expression of STING, IRF3, P-IRF3, and Bax proteins were assessed by immunoblotting on monocytes transfected with HIV-1 $ssDNA_{90}$ for 3 hr.

(B and C) STING pull-down (B) and anti-Bax co-IP (C) were performed on monocytes transfected with HIV-1 $ssDNA_{90}$ (n = 3).

(D) Monocytes treated with HIV-1 $ssDNA_{90}$ displayed higher levels of mitochondria-dependent apoptosis. At 48 hpi, levels of Annexin-V, mitochondria depolarization (% of $DiOC_6(3)^{low}$ cells), and costaining were assessed on gated $CD14^+$ monocytes in the presence of HIV-1 RTI. Results show the percentages of HIV-1-induced apoptosis and Bax expression, determined by the formula: % of staining in HIV-1 RTI-transfected monocytes − % of staining in monocytes electroporated alone. Flow histograms shown on the right are representative of raw data from five independent experiments. Data are represented as mean ± SD. See related Figure S6.

triggering apoptosis, a biotinylated 90 nt ss or ds RTI from the U5 region of HTLV-1 was introduced into monocytes, and it triggered apoptosis in a manner similar to infection.

One of the outstanding questions raised by these studies is: how does SAMHD1-mediated restriction of retroviral replication initiate apoptosis and impact the host innate response to retroviral infection? Our experiments provide evidence that the endoplasmic reticulum resident adaptor STING triggers both processes through IRF3 activation. STING is known to regulate type I IFN immunity following recognition of pathogen DNA (Ishikawa et al., 2009); its ability to directly interact with viral DNA was characterized recently, and STING was shown to be the primary sensor involved in DNA recognition (Abe et al., 2013). Although STING was readily pulled down in complex with RTI, we cannot exclude the involvement of other DNA sensors such as MRE11 (Kondo et al., 2013), DDX41 (Zhang et al., 2011), or IFI16 (Unterholzner et al., 2010). Importantly, the DNA sensor cGAS was recently shown to sense HIV-1 and other retroviruses via the recognition of retroviral DNA reverse transcriptase intermediates, leading to STING-mediated activation of IRF3-dependent antiviral activity (Gao et al. 2013; Sun et al., 2013). The release of type 1 IFN and/or proinflammatory cytokines during HTLV-1 infection could also contribute to the induction of apoptosis in monocytes.

Complex formation between STING and HTLV-1 RTI initiated apoptosis through the formation of an IRF3-Bax complex (Chattopadhyay et al., 2010, 2013). Following HTLV-1 infection of monocytes, we detected an IRF3-Bax complex formation that was abrogated in monocytes when STING expression was silenced, thus identifying STING signaling as an additional pathway involved in IRF3-Bax induction. That IRF3 activation can promote both apoptotic and antiviral signaling was demonstrated in earlier studies in which constitutively active forms of IRF3 and IRF7 were transduced into primary macrophages (Goubau et al., 2009). Transcriptional profiling and biological characterization of transduced human macrophages demonstrated that IRF3 initiated an antiviral response, but also rapidly induced cell death through the upregulation of a subset of proapoptotic genes (Goubau et al., 2009).

We observed similar apoptotic mechanisms associated with STING binding and IRF3-Bax induction of apoptosis when HIV-1 RTI were introduced into monocytes, arguing in favor of the generality of the SAMHD1-STING initiation of apoptotic signaling in human retroviral infection (Figure 7). This observation, however, is not applicable in the context of HIV-2 that expresses Vpx; the physical interaction of SAMHD1 with Vpx recruits the Cul4-DDB1-DCAF1 complex to drive its proteasomal degradation (Descours et al., 2012; Laguette et al., 2011; Lahouassa

et al., 2012). Furthermore, the exonuclease TREX1 suppresses recognition of HIV-1 replicative intermediates by STING as a viral evasion mechanism (Yan et al., 2010).

No correlation was observed between HTLV-1-induced apoptosis and expression levels of SAMHD1 (data not shown), consistent with studies where HIV-1 restriction was not solely associated with SAMHD1 expression levels (Descours et al., 2012). In fact, monocyte-derived DC are productively infected by HTLV-1 (Abe et al., 2013; Jones et al., 2008), despite SAMHD1 expression (Laguette et al., 2011). Moreover, in macrophages and cycling $CD4^+$ T cells, HTLV-1 infection was not blocked by SAMHD1 and led to Tax production (Gramberg et al., 2013), indicating that SAMHD1 function differs in other cell contexts. It is likely that regulation of SAMHD1 restriction depends on several retroviral and host parameters including posttranslational modifications, cellular cofactors, and splice variations (Descours et al., 2012; Welbourn et al., 2012). In this regard, it was recently demonstrated that SAMHD1 activity is modulated by phosphorylation status. Cyclin A2/CDK1 phosphorylated SAMHD1 at Thr592 SAMHD1 in cycling cells, and phosphorylation at Thr592 correlated with loss of restriction (Cribier et al., 2013; White et al., 2013). Furthermore, type 1 IFN treatment reduced Thr592 phosphorylation, indicating a link between SAMHD1 phosphorylation, antiviral activity, and innate immune signaling (Cribier et al., 2013). A Thr592 phosphomimetic SAMHD1 mutant did not restrict HIV-1 replication, despite dNTPase activity, oligomer formation, and nuclear localization (White et al., 2013). These experiments identify phosphorylation of SAMHD1 at Thr592 by cyclin A2/CDK1 as an important regulatory mechanism and highlight the need for further studies to elucidate the mechanisms that regulate SAMHD1 activity and function.

The demonstration that cytoplasmic RTI contributes to the elimination of HTLV-1-infected monocytes may have important consequences for human retroviral pathogenesis. The clearance of infected monocytes may prevent transmission to $CD4^+$ T cells, and may also deplete the precursor pool of myeloid dendritic cells that play a crucial role in controlling HTLV-1 infection (Rahman et al., 2011). Individuals suffering from ATL or HAM/TSP possess a lower absolute number of DC than healthy individuals (Azakami et al., 2009; Hishizawa et al., 2004), and HTLV-1-infected monocytes also exhibit defective differentiation into DC (Makino et al., 2000; Nascimento et al., 2011). These factors may influence the development of HAM/TSP or ATL in HTLV-1 infected individuals, thus emphasizing the need to better understand the early host restriction of HTLV-1 infectivity by SAMHD1.

EXPERIMENTAL PROCEDURES

Products

RPMI-1640 media, FBS, and antibiotics were provided by Wisent Technologies. All monoclonal antibodies (mAbs) and products used for flow cytometry were purchased from Biolegend, except for anti-cleaved caspase-3-PE mAbs, Annexin-V buffer 10X, and Annexin-V-V450 obtained from Becton Dickinson. Anti-p19 mAbs (clone TP-7) was purchased from ZeptoMetrix Corporation, whereas anti-gp46 mAbs (clone 67/5.5.13.1) was purchased from Abcam. Anti-Tax-FITC mAbs (clone LT4) was generously provided by Dr. Yuetsu Tanaka (Kitasato University, Kanagawa, Japan). All antibodies included in western blotting analyses came from Cell signaling Biotechnology Inc., except for anti-Bax mAbs (Santa Cruz Biotechnology Inc.). Pan-caspase inhibitor Z-VAD-FMK (Z-VAD) was purchased from R&D Systems. All cell lines were obtained from the ATCC.

Purification of Monocytes

Leukaphereses from healthy donors were obtained from the Royal Victoria Hospital, Montreal (QC, Canada), with informed consent of the patients and in agreement with the Royal Victoria Hospital, the Jewish General Hospital, and McGill University Research Ethics Committee.

HTLV-1 Purification and In Vitro Infection

HTLV-1 viruses were purified from MT-2 supernatants. Cells were seeded overnight in complete RPMI (2×10^6 cells/ml). Supernatants were collected and ultracentrifuged for 2 hr at 30,000× *g* at 4°C. The viral pellet was resuspended in complete RPMI, and HTLV-1 particles were quantified by gag p19 ELISA assays (ZeptoMetrix). A total of 200,000 purified monocytes were incubated with 2 μg HTLV-1 for 3 hr at 37°C in 0.5 ml RPMI complete with or without 100 μM Z-VAD-FMK. To specifically block HTLV-1 infection, neutralizing anti-gp46 mAbs (at 10 μg/ml; Abcam) were incubated 30 min at 4°C with HTLV-1 prior in vitro infection. At 3 hpi, monocytes were washed twice in complete RPMI and then cocultured with 8×10^5 autologous monocyte-depleted PBMCs (1 ml complete RPMI; [HTLV-1] = 2 μg/ml).

Western Blotting

Protein lysates (2–10 μg) from monocytes were subjected to western blot analysis as previously described (Olière et al., 2010).

Small Interfering RNA Assays

A total of 10^7 purified monocytes were electroporated in the presence of control or specific siRNA using Nucleofactor II technology according the manufacturer's protocol (Amaxa human monocyte nucleofactor kit).

Biotinylated Retroviral DNA_{90} Assay

Retroviral DNA was produced by Integrated DNA Technologies. HTLV-1 $ssDNA_{90}$ is the reverse complement of the 5′ UTR region (315–404 of complete HTLV-1 genome; NCBI) that is 90 bases long and conjugated with biotin on the 5′ end. A total of 10^7 monocytes were transfected with 10 μg $vDNA_{90}$ for 24 hr in RPMI + 30% FBS in the absence of antibiotics. Monocytes were washed and then cocultured in complete RPMI with $CD14^{neg}$ PBMCs.

STING Pull-Down and Bax Coimmunoprecipitation

Monocytes were infected with HTLV-1 or transfected with biotinylated RTI for 6 hr (pull-down) or 3 hr (co-IP). Monocytes were lysed using CHAPS buffer with protease inhibitors as previously described (Samuel et al., 2010). Protein (3 μg) was collected and referred to as the "input" fraction.

Statistical Analysis

Statistical analyses were performed using the nonparametric Mann-Whitney U test, assuming independent samples. However, differences among the treatment groups performed with n = 3 samples were analyzed by the parametric unpaired Student's t test. P values of less than 0.05 were considered statistically significant. ***, $p < 0.001$; **, $p < 0.01$, and *, $p < 0.05$.

SUPPLEMENTAL INFORMATION

Supplemental Information includes six figures, one table, and Supplemental Experimental Procedures and can be found with this article online at http://dx.doi.org/10.1016/j.chom.2013.09.009.

AUTHOR CONTRIBUTIONS

A.S. performed most of the experiments and helped write the paper; S.M.B. and R.L. aided in the STING pull-down and anti-Bax coimmunoprecipitation experiments; D.O. helped to write the paper and edited text and figures; J.H. and J.v.G. conceived the study, designed experiments, supervised the experiments, and wrote the paper.

ACKNOWLEDGMENTS

We are grateful to the donors who participated in this study, as well as Dr. J.P. Routy, Royal Victoria Hospital and the attending staff. This project was supported by research funds from VGTI Florida and the Canadian Institutes of Health Research (#MOP-106686).

Received: July 8, 2013
Revised: August 28, 2013
Accepted: September 24, 2013
Published: October 16, 2013

REFERENCES

Abe, T., Harashima, A., Xia, T., Konno, H., Konno, K., Morales, A., Ahn, J., Gutman, D., and Barber, G.N. (2013). STING recognition of cytoplasmic DNA instigates cellular defense. Mol. Cell *50*, 5–15.

Ayinde, D., Casartelli, N., and Schwartz, O. (2012). Restricting HIV the SAMHD1 way: through nucleotide starvation. Nat. Rev. Microbiol. *10*, 675–680.

Azakami, K., Sato, T., Araya, N., Utsunomiya, A., Kubota, R., Suzuki, K., Hasegawa, D., Izumi, T., Fujita, H., Aratani, S., et al. (2009). Severe loss of invariant NKT cells exhibiting anti-HTLV-1 activity in patients with HTLV-1-associated disorders. Blood *114*, 3208–3215.

Baldauf, H.M., Pan, X., Erikson, E., Schmidt, S., Daddacha, W., Burggraf, M., Schenkova, K., Ambiel, I., Wabnitz, G., Gramberg, T., et al. (2012). SAMHD1 restricts HIV-1 infection in resting CD4(+) T cells. Nat. Med. *18*, 1682–1687.

Barber, G.N. (2011). Innate immune DNA sensing pathways: STING, AIMII and the regulation of interferon production and inflammatory responses. Curr. Opin. Immunol. *23*, 10–20.

Berger, A., Sommer, A.F., Zwarg, J., Hamdorf, M., Welzel, K., Esly, N., Panitz, S., Reuter, A., Ramos, I., Jatiani, A., et al. (2011). SAMHD1-deficient CD14+ cells from individuals with Aicardi-Goutières syndrome are highly susceptible to HIV-1 infection. PLoS Pathog. *7*, e1002425.

Blasius, A.L., and Beutler, B. (2010). Intracellular toll-like receptors. Immunity *32*, 305–315.

Burdette, D.L., and Vance, R.E. (2013). STING and the innate immune response to nucleic acids in the cytosol. Nat. Immunol. *14*, 19–26.

Chattopadhyay, S., Marques, J.T., Yamashita, M., Peters, K.L., Smith, K., Desai, A., Williams, B.R., and Sen, G.C. (2010). Viral apoptosis is induced by IRF-3-mediated activation of Bax. EMBO J. *29*, 1762–1773.

Chattopadhyay, S., Yamashita, M., Zhang, Y., and Sen, G.C. (2011). The IRF-3/Bax-mediated apoptotic pathway, activated by viral cytoplasmic RNA and DNA, inhibits virus replication. J. Virol. *85*, 3708–3716.

Chattopadhyay, S., Fensterl, V., Zhang, Y., Veleeparambil, M., Yamashita, M., and Sen, G.C. (2013). Role of interferon regulatory factor 3-mediated apoptosis in the establishment and maintenance of persistent infection by Sendai virus. J. Virol. *87*, 16–24.

Colisson, R., Barblu, L., Gras, C., Raynaud, F., Hadj-Slimane, R., Pique, C., Hermine, O., Lepelletier, Y., and Herbeuval, J.P. (2010). Free HTLV-1 induces TLR7-dependent innate immune response and TRAIL relocalization in killer plasmacytoid dendritic cells. Blood *115*, 2177–2185.

Cook, L.B., Elemans, M., Rowan, A.G., and Asquith, B. (2013). HTLV-1: persistence and pathogenesis. Virology *435*, 131–140.

Cribier, A., Descours, B., Valadão, A.L., Laguette, N., and Benkirane, M. (2013). Phosphorylation of SAMHD1 by cyclin A2/CDK1 regulates its restriction activity toward HIV-1. Cell Rep *3*, 1036–1043.

Descours, B., Cribier, A., Chable-Bessia, C., Ayinde, D., Rice, G., Crow, Y., Yatim, A., Schwartz, O., Laguette, N., and Benkirane, M. (2012). SAMHD1 restricts HIV-1 reverse transcription in quiescent CD4(+) T-cells. Retrovirology *9*, 87.

Doitsh, G., Cavrois, M., Lassen, K.G., Zepeda, O., Yang, Z., Santiago, M.L., Hebbeler, A.M., and Greene, W.C. (2010). Abortive HIV infection mediates CD4 T cell depletion and inflammation in human lymphoid tissue. Cell *143*, 789–801.

Gao, D., Wu, J., Wu, Y.T., Du, F., Aroh, C., Yan, N., Sun, L., and Chen, Z.J. (2013). Cyclic GMP-AMP synthase is an innate immune sensor of HIV and other retroviruses. Science *341*, 903–906.

Goldstone, D.C., Ennis-Adeniran, V., Hedden, J.J., Groom, H.C., Rice, G.I., Christodoulou, E., Walker, P.A., Kelly, G., Haire, L.F., Yap, M.W., et al. (2011). HIV-1 restriction factor SAMHD1 is a deoxynucleoside triphosphate triphosphohydrolase. Nature *480*, 379–382.

Goubau, D., Romieu-Mourez, R., Solis, M., Hernandez, E., Mesplède, T., Lin, R., Leaman, D., and Hiscott, J. (2009). Transcriptional re-programming of primary macrophages reveals distinct apoptotic and anti-tumoral functions of IRF-3 and IRF-7. Eur. J. Immunol. *39*, 527–540.

Gramberg, T., Kahle, T., Bloch, N., Wittmann, S., Müllers, E., Daddacha, W., Hofmann, H., Kim, B., Lindemann, D., and Landau, N.R. (2013). Restriction of diverse retroviruses by SAMHD1. Retrovirology *10*, 26.

Hishizawa, M., Imada, K., Kitawaki, T., Ueda, M., Kadowaki, N., and Uchiyama, T. (2004). Depletion and impaired interferon-alpha-producing capacity of blood plasmacytoid dendritic cells in human T-cell leukaemia virus type I-infected individuals. Br. J. Haematol. *125*, 568–575.

Hollenbaugh, J.A., Gee, P., Baker, J., Daly, M.B., Amie, S.M., Tate, J., Kasai, N., Kanemura, Y., Kim, D.H., Ward, B.M., et al. (2013). Host factor SAMHD1 restricts DNA viruses in non-dividing myeloid cells. PLoS Pathog. *9*, e1003481.

Igakura, T., Stinchcombe, J.C., Goon, P.K., Taylor, G.P., Weber, J.N., Griffiths, G.M., Tanaka, Y., Osame, M., and Bangham, C.R. (2003). Spread of HTLV-I between lymphocytes by virus-induced polarization of the cytoskeleton. Science *299*, 1713–1716.

Ishikawa, H., and Barber, G.N. (2008). STING is an endoplasmic reticulum adaptor that facilitates innate immune signalling. Nature *455*, 674–678.

Ishikawa, H., Ma, Z., and Barber, G.N. (2009). STING regulates intracellular DNA-mediated, type I interferon-dependent innate immunity. Nature *461*, 788–792.

Jones, K.S., Petrow-Sadowski, C., Bertolette, D.C., Huang, Y., and Ruscetti, F.W. (2005). Heparan sulfate proteoglycans mediate attachment and entry of human T-cell leukemia virus type 1 virions into CD4+ T cells. J. Virol. *79*, 12692–12702.

Jones, K.S., Petrow-Sadowski, C., Huang, Y.K., Bertolette, D.C., and Ruscetti, F.W. (2008). Cell-free HTLV-1 infects dendritic cells leading to transmission and transformation of CD4(+) T cells. Nat. Med. *14*, 429–436.

Kaushik, R., Zhu, X., Stranska, R., Wu, Y., and Stevenson, M. (2009). A cellular restriction dictates the permissivity of nondividing monocytes/macrophages to lentivirus and gammaretrovirus infection. Cell Host Microbe *6*, 68–80.

Kawai, T., and Akira, S. (2011). Toll-like receptors and their crosstalk with other innate receptors in infection and immunity. Immunity *34*, 637–650.

Kim, B., Nguyen, L.A., Daddacha, W., and Hollenbaugh, J.A. (2012). Tight interplay among SAMHD1 protein level, cellular dNTP levels, and HIV-1 proviral DNA synthesis kinetics in human primary monocyte-derived macrophages. J. Biol. Chem. *287*, 21570–21574.

Kondo, T., Kobayashi, J., Saitoh, T., Maruyama, K., Ishii, K.J., Barber, G.N., Komatsu, K., Akira, S., and Kawai, T. (2013). DNA damage sensor MRE11 recognizes cytosolic double-stranded DNA and induces type I interferon by regulating STING trafficking. Proc. Natl. Acad. Sci. USA *110*, 2969–2974.

Kumar, H., Kawai, T., and Akira, S. (2011). Pathogen recognition by the innate immune system. Int. Rev. Immunol. *30*, 16–34.

Laguette, N., and Benkirane, M. (2012). How SAMHD1 changes our view of viral restriction. Trends Immunol. *33*, 26–33.

Laguette, N., Sobhian, B., Casartelli, N., Ringeard, M., Chable-Bessia, C., Ségéral, E., Yatim, A., Emiliani, S., Schwartz, O., and Benkirane, M. (2011). SAMHD1 is the dendritic- and myeloid-cell-specific HIV-1 restriction factor counteracted by Vpx. Nature *474*, 654–657.

Laguette, N., Rahm, N., Sobhian, B., Chable-Bessia, C., Münch, J., Snoeck, J., Sauter, D., Switzer, W.M., Heneine, W., Kirchhoff, F., et al. (2012). Evolutionary and functional analyses of the interaction between the myeloid restriction factor SAMHD1 and the lentiviral Vpx protein. Cell Host Microbe *11*, 205–217.

Lahouassa, H., Daddacha, W., Hofmann, H., Ayinde, D., Logue, E.C., Dragin, L., Bloch, N., Maudet, C., Bertrand, M., Gramberg, T., et al. (2012). SAMHD1

restricts the replication of human immunodeficiency virus type 1 by depleting the intracellular pool of deoxynucleoside triphosphates. Nat. Immunol. *13*, 223–228.

Makino, M., Wakamatsu, S., Shimokubo, S., Arima, N., and Baba, M. (2000). Production of functionally deficient dendritic cells from HTLV-I-infected monocytes: implications for the dendritic cell defect in adult T cell leukemia. Virology *274*, 140–148.

Nascimento, C.R., Lima, M.A., de Andrada Serpa, M.J., Espindola, O., Leite, A.C., and Echevarria-Lima, J. (2011). Monocytes from HTLV-1-infected patients are unable to fully mature into dendritic cells. Blood *117*, 489–499.

Nisole, S., and Saïb, A. (2004). Early steps of retrovirus replicative cycle. Retrovirology *1*, 9.

Olière, S., Hernandez, E., Lézin, A., Arguello, M., Douville, R., Nguyen, T.L., Olindo, S., Panelatti, G., Kazanji, M., Wilkinson, P., et al. (2010). HTLV-1 evades type I interferon antiviral signaling by inducing the suppressor of cytokine signaling 1 (SOCS1). PLoS Pathog. *6*, e1001177.

Pais-Correia, A.M., Sachse, M., Guadagnini, S., Robbiati, V., Lasserre, R., Gessain, A., Gout, O., Alcover, A., and Thoulouze, M.I. (2010). Biofilm-like extracellular viral assemblies mediate HTLV-1 cell-to-cell transmission at virological synapses. Nat. Med. *16*, 83–89.

Ragin, C., Edwards, R., Heron, D.E., Kuo, J., Wentzel, E., Gollin, S.M., and Taioli, E. (2008). Prevalence of cancer-associated viral infections in healthy afro-Caribbean populations: a review of the literature. Cancer Invest. *26*, 936–947.

Rahman, S., Khan, Z.K., Wigdahl, B., Jennings, S.R., Tangy, F., and Jain, P. (2011). Murine FLT3 ligand-derived dendritic cell-mediated early immune responses are critical to controlling cell-free human T cell leukemia virus type 1 infection. J. Immunol. *186*, 390–402.

Rice, G.I., Bond, J., Asipu, A., Brunette, R.L., Manfield, I.W., Carr, I.M., Fuller, J.C., Jackson, R.M., Lamb, T., Briggs, T.A., et al. (2009). Mutations involved in Aicardi-Goutières syndrome implicate SAMHD1 as regulator of the innate immune response. Nat. Genet. *41*, 829–832.

Samuel, S., Tumilasci, V.F., Oliere, S., Nguyên, T.L., Shamy, A., Bell, J., and Hiscott, J. (2010). VSV oncolysis in combination with the BCL-2 inhibitor obatoclax overcomes apoptosis resistance in chronic lymphocytic leukemia. Mol. Ther. *18*, 2094–2103.

Sun, L., Wu, J., Du, F., Chen, X., and Chen, Z.J. (2013). Cyclic GMP-AMP synthase is a cytosolic DNA sensor that activates the type I interferon pathway. Science *339*, 786–791.

Triques, K., and Stevenson, M. (2004). Characterization of restrictions to human immunodeficiency virus type 1 infection of monocytes. J. Virol. *78*, 5523–5527.

Unterholzner, L., Keating, S.E., Baran, M., Horan, K.A., Jensen, S.B., Sharma, S., Sirois, C.M., Jin, T., Latz, E., Xiao, T.S., et al. (2010). IFI16 is an innate immune sensor for intracellular DNA. Nat. Immunol. *11*, 997–1004.

Van Prooyen, N., Gold, H., Andresen, V., Schwartz, O., Jones, K., Ruscetti, F., Lockett, S., Gudla, P., Venzon, D., and Franchini, G. (2010). Human T-cell leukemia virus type 1 p8 protein increases cellular conduits and virus transmission. Proc. Natl. Acad. Sci. USA *107*, 20738–20743.

Verdonck, K., González, E., Van Dooren, S., Vandamme, A.M., Vanham, G., and Gotuzzo, E. (2007). Human T-lymphotropic virus 1: recent knowledge about an ancient infection. Lancet Infect. Dis. *7*, 266–281.

Welbourn, S., Miyagi, E., White, T.E., Diaz-Griffero, F., and Strebel, K. (2012). Identification and characterization of naturally occurring splice variants of SAMHD1. Retrovirology *9*, 86.

White, T.E., Brandariz-Nuñez, A., Valle-Casuso, J.C., Amie, S., Nguyen, L.A., Kim, B., Tuzova, M., and Diaz-Griffero, F. (2013). The retroviral restriction ability of SAMHD1, but not its deoxynucleotide triphosphohydrolase activity, is regulated by phosphorylation. Cell Host Microbe *13*, 441–451.

Yamano, Y., and Sato, T. (2012). Clinical pathophysiology of human T-lymphotropic virus-type 1-associated myelopathy/tropical spastic paraparesis. Front Microbiol *3*, 389.

Yan, N., Regalado-Magdos, A.D., Stiggelbout, B., Lee-Kirsch, M.A., and Lieberman, J. (2010). The cytosolic exonuclease TREX1 inhibits the innate immune response to human immunodeficiency virus type 1. Nat. Immunol. *11*, 1005–1013.

Zhang, Z., Yuan, B., Bao, M., Lu, N., Kim, T., and Liu, Y.J. (2011). The helicase DDX41 senses intracellular DNA mediated by the adaptor STING in dendritic cells. Nat. Immunol. *12*, 959–965.

Zhong, B., Yang, Y., Li, S., Wang, Y.Y., Li, Y., Diao, F., Lei, C., He, X., Zhang, L., Tien, P., and Shu, H.B. (2008). The adaptor protein MITA links virus-sensing receptors to IRF3 transcription factor activation. Immunity *29*, 538–550.